Quaternary Research 82 (2014) 121–131

Contents lists available at ScienceDirect

Quaternary Research

journal homepage: www.elsevier.com/locate/yqres

Identification of a Holocene aquifer–lagoon system using hydrogeochemical data

F. Sola [a,*], A. Vallejos [a], L. Daniele [b,c], A. Pulido-Bosch [a]

[a] Water Resources and Environmental Geology, University of Almería, Spain
[b] Department of Geology, FCFM, University of Chile, Chile
[c] Andean Geothermal Center of Excellence (CEGA), Fondap-Conicyt 15090013, Chile

ARTICLE INFO

Article history:
Received 23 October 2013
Available online 9 May 2014

Keywords:
Hydrochemistry
Stable isotopes
Paleowaters
Coastal aquifer
Middle Holocene

ABSTRACT

The hydrogeochemical characteristics of the Cabo de Gata coastal aquifer (southeastern Spain) were studied in an attempt to explain the anomalous salinity of its groundwater. This detritic aquifer is characterised by the presence of waters with highly contrasting salinities; in some cases the salinity exceeds that of seawater. Multivariate analysis of water samples indicates two groups of water (G1 and G2). Group G1 is represented in the upper part of the aquifer, where the proportion of seawater varies between 10 and 60%, whilst G2 waters, taken from the lower part of the aquifer, contain 60−70% seawater. In addition, hydrogeochemical modelling was applied, which reveals that the waters have been subject to evaporation between 25 and 35%. There was a good agreement between the modelled results and the observed water chemistry. This evaporation would have occurred during the Holocene, in a coastal lagoon environment; the resulting brines would have infiltrated into the aquifer and, due to their greater density, sunk towards the impermeable base. The characteristics of this water enabled us to reconstruct the interactions that must have occurred between the coastal aquifer and the lagoon, and to identify the environmental conditions that prevailed in the study area during the Middle Holocene.

Introduction

The movement of groundwater within an aquifer can be extremely slow, occurring over geological time scales. Rather than being a function solely of the current physical setting, therefore, groundwater salinity can be a product of previous sea-level fluctuations, subsidence, tectonic events and previous climates. Unconsolidated superficial aquifers have formed in many coastal areas in the Holocene — over the last 10 ka. Many coastal areas have been subject to multiple phases of marine transgression, and the distinction between modern and relict seawater intrusion is an important objective of many studies (Darling et al., 1997; Petalas and Diamantis, 1999). The salinity of the fresh water and salt water can have many and varied sources (Stuyfzand and Stuurman, 1994; Custodio, 1997; Custodio, 2010; Werner et al., 2013), which commonly include seawater intrusion due to overexploitation of the aquifer, presence of fossil seawater from earlier flood events, evaporation, and dissolution of salt deposits.

Otherwise, the mixing of process of different waters along flow paths combined with evaporation, vegetation transpiration and dissolution of salt mineral may also lead to salinity increase (Faye et al., 2005) For instance, the transpiration could increase the salinity of the residual water. If the source water is sea water, then the residual water may become highly saline (Fass et al., 2007).

* Corresponding author.
E-mail address: fesola@ual.es (F. Sola).

Sea-level fluctuations throughout the Quaternary affected coastal aquifers all over the world (Edmunds and Milne, 2001; Han et al., 2011; Wang and Jiao, 2012), causing them to become salinized. After the larger variations in sea level at the end of the Last Glacial, these salts have been washed, although in confined or low-permeability coastal aquifers part of the saline water can be retained (Post, 2003).

Coastal aquifers are characterized by the presence of a mixing zone containing both continental fresh water and seawater. The position and extent of this mixing zone are determined by a variety of factors, including the permeability of the aquifer matrix, layer thickness, the piezometric head and density differences between the fresh water and salt water. Also, the mixing zone is influenced by K variability/heterogeneity, not just the value itself (Lu et al., 2013). Molecular diffusion and dispersion are also important for slow moving wedges (Kooi et al., 2000). A special case is where there is also interaction of the coastal aquifer with a continental water body, such as a lagoon. In such cases, the aquifer–lagoon interconnection complicates the hydrodynamic model but the origin of the groundwater can still be identified from its geochemical signal (Gattacceca et al., 2009; Kharroubi et al., 2012; Re et al., 2013; Sánchez-Martos et al., 2014). Over geological time, the position of the fresh water–seawater interface will have been affected by relative changes in sea level (Yechieli et al., 2010; Kafri and Yechieli, 2012; Været et al., 2012). There are few published studies of the characteristics of old saline wedges (Manzano et al., 2001; Akouvi et al., 2008; Cheikh et al., 2012), but it is clear that

http://dx.doi.org/10.1016/j.yqres.2014.04.012
0033-5894/

similar techniques can be used to study both former and present-day mixing zones.

The tools to characterise water bodies with different salinities can be diverse, thereby in a groundwater system with several water bodies of different salinities, the mixing fractions can generally be calculated by conservative species such as the chloride ion (Sola et al., 2013). Environmental stable ($\delta^{18}O$, $\delta^{2}H$, $\delta^{13}C$) and radioactive (^{3}H and ^{14}C) isotopes, together with geochemical data are used to identify the origin of salinisation in different environments (Sukhija et al., 1996; Carreira et al., 2014). So, the use of ^{14}C distinguishes bodies characterized by different salinities, which could be relics from an ancient hydrological system (Avrahamov et al., 2010).

Sometimes it is possible to detect the existence of hypersaline water within an aquifer, which cannot be explained using a standard seawater intrusion model (Hodgkinson et al., 2007). Evaporative concentration of seawater is perhaps the most commonly cited mechanism for the formation of natural brines. In settings where direct geological evidence for large-scale evaporation is absent, however, alternative mechanisms must be considered. For example, Frank et al. (2010) explain the presence of brine in high-latitude involving the concentration of seawater via freezing along the margins of Pleistocene ice sheets.

The present study focuses on a hydrogeochemical and isotopic analysis of a coastal aquifer in the south-eastern Iberian Peninsula, with the aim of determining the source of its anomalous groundwater salinity. Palaeo-marine intrusion was detected and, using the available hydrogeochemical information, we have reconstructed the environmental conditions that prevailed in a coastal lagoon environment, to which this palaeo-marine intrusion was linked.

Study area

The Cabo de Gata area is located in south-eastern Spain, and forms part of the Betic Cordillera. The study area corresponds to the small coastal aquifer of Cabo de Gata, which has a surface area of only 16 km^2. It is delimited to the east by the volcanic rocks of the Sierra of Cabo de Gata, to the west, by the Carboneras Fault, and to the south, by the Mediterranean Sea (Fig. 1A).

The arid climate is the most significant feature of this area; it falls into the Mediterranean subdesert domain. Mean insolation is high — around 2960 h/yr, and the Cabo de Gata area has the lowest rainfall of the Iberian Peninsula (170 mm/yr recorded at the Cabo lighthouse station). The temperature regime is mild, with mean temperatures of between 15 and 22°C, and a minimum that does not dip below 12°C. All these features determine its subdesertic climate type. The distribution of precipitation through the year is restricted to ten or twenty days, linked to favourable periods in the autumn and winter. This means that, on occasions, more than 40% of the annual total can fall in a single day.

The aquifer is highly compartmentalized by faults that cut through the Plio-Quaternary deposits. There are two main faults, the Carboneras Fault, oriented N40°E, and a conjugate fault that runs parallel to the coast. The surface of the aquifer consists mainly of marine terraces composed of Upper Pleistocene conglomerates (Hillaire-Marcel et al., 1986), which are partly covered by Holocene and present-day sand-dune belts. To the north, these deposits give way to silts and clays; these lie in a depression interpreted to be a former lagoon (Fig. 1A) dating to between 8 and 3 ka (Goy et al., 1998). Nowadays, this lagoon appears only to the east (Fig. 1A) which, given the high evaporation rate in the area, is used for commercial salt extraction.

The impermeable base of the aquifer comprises Pliocene silts lying at 80 m depth. The aquifer is multi-layer, formed by Plio-Quaternary sands and conglomerates, which means that the unconfined aquifer becomes semi-confined towards its base (Fig. 2). Six boreholes have been drilled in this area (R1 to R6), three of which supply saline water to a desalination plant; the other three are out of operation at the moment, though they were drilled for the same purpose. The boreholes that supply the desalination plant lie 400 m from the shore (Fig. 1B) and have a single slotted length at their base of the aquifer. The water extracted has a conductivity of 55 to 60 mS/cm (Daniele et al., 2011). Transmissivity, calculated from a pumping test in October 2006, varies from 1000 to 2000 m^2/day.

The transition zone within the long-perforated boreholes can be affected by tidal oscillations, which cause vertical flow within the borehole that does not exist in the aquifer, modifying the behaviour of the transition zone in the aquifer. Measurements within short-perforated boreholes show that this kind of borehole diminishes the distortion dramatically. Therefore, short-perforation measurements should be considered to be more representative monitoring of the aquifer (Levanon et al., 2013). The piezometer network in the study area to monitor the evolution of marine intrusion, comprises two piezometers, slotted along their whole length, plus two clusters of each with three piezometers. The fully slotted piezometers (P-1 and P-2) are 80 m deep, whilst the multi-piezometers (MP-1 and MP-2) have different depths and are slotted only at their base, which coincides with the aquifer layers that are delimited by the silt beds (Fig. 2).

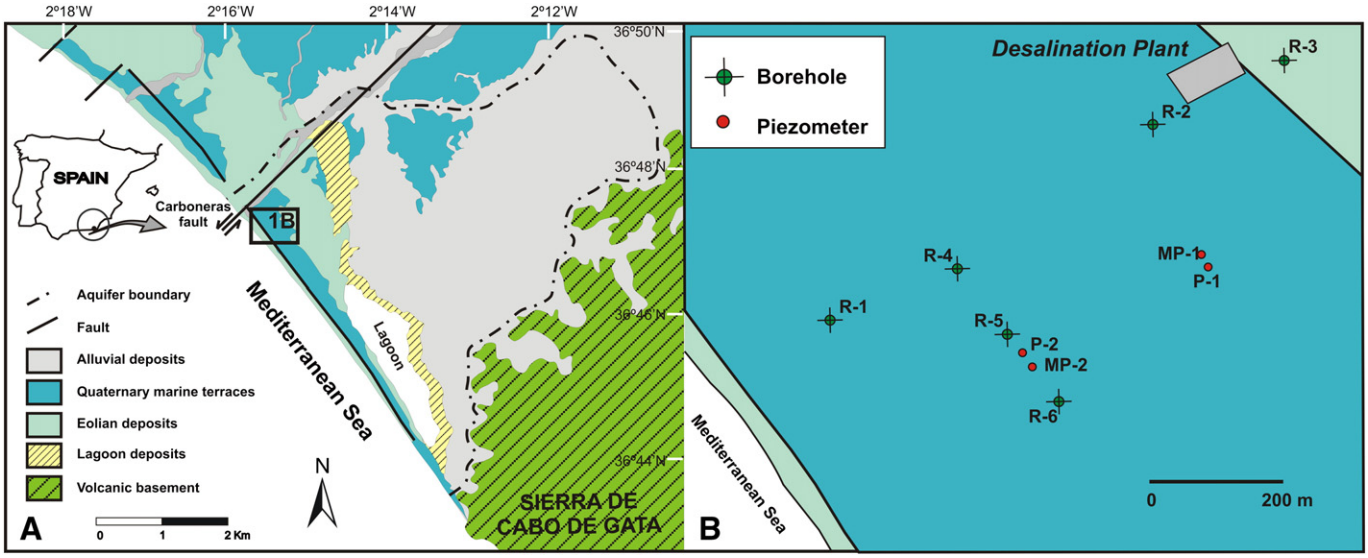

Figure 1. Geological scheme (A) and location of the study area and monitoring points (B).

https://doi.org/10.1016/j.yqres.2014.04.012 Published online by Cambridge University Press

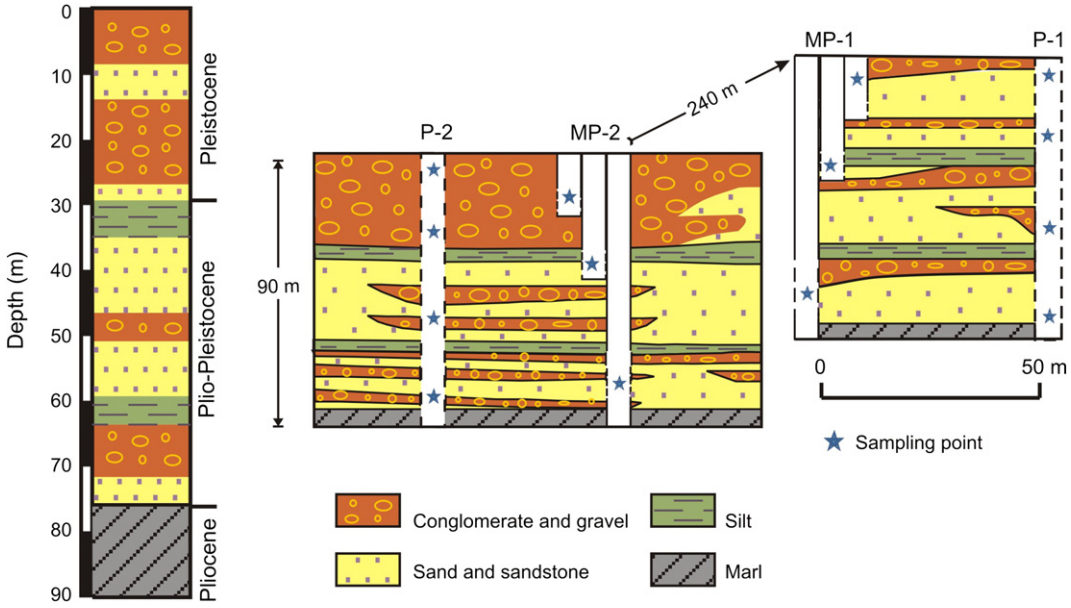

Figure 2. Simplified lithological column and hydrogeological scheme including the sampling points.

Materials and methods

In order to determine the processes influencing groundwater salinity in the aquifer, a monitoring network was established in May 2008 (Fig. 1B). Groundwater samples were taken from the single piezometers (P-1, P-2) and from the two piezometer clusters (MP-1, MP-2). The clusters are short-screened, each piezometer penetrating only one of the three water layers (fresh, mixed and seawater). The multi-level sampling technique was used to collect groundwater samples from the top to the bottom of the piezometers using a discrete interval sampler (Solinst Mod. 425). A representative seawater sample was taken near the coast, as well as a representative fresh-water sample from the aquifer.

Temperature, electrical conductivity and pH were determined in situ. Alkalinity (as HCO_3^-) was determined by titration at the time of sampling. Samples were taken in duplicate, filtered using a 0.45 μm Millipore filter and stored in polyethylene bottles at 4°C. For metal analysis, to avoid absorption or precipitation, the samples were acidified to pH <2 with environmental grade (ultra pure) nitric acid. Sample composition was determined using an ICP-Mass Spectrometer (Acme Labs, Vancouver, Canada). Environmental water isotopes (^{18}O and deuterium) were also analysed (Stable Isotope Laboratory, Interdepartmental Research Service (SIDI), Autonomous University of Madrid). Isotope ratios were measured using an IRMS (Isotope Ratio Mass Spectrometer). The standard used was the Vienna Standard Mean Ocean Water (VSMOW). Analytical uncertainty was ±0.2 for $\delta^{18}O$, and ±0.1 for δ^2H.

Groundwater levels in the monitoring network were measured during a period when the desalination plant was extracting water from the aquifer intermittently, so measurements were made at times both with and without pumping. During this period, vertical logs of temperature and conductivity were directly determined in the field using a temperature-conductivity multi-meter (Solinst 107 TLC metre).

Assuming chloride and ^{18}O are conservative ions (Ci), the percentage of seawater in a sample can be calculated using the mass balance, assuming conservative mixing of seawater and fresh water (Appelo and Postma, 2005), described by the following formula:

$$\text{Seawater}(\%) = \left[\text{Ci}_{\text{sample}} - \text{Ci}_{\text{fresh}}\right] / \left[\text{Ci}_{\text{sea}} - \text{Ci}_{\text{fresh}}\right] \times 100.$$

The ionic delta values (Δ) for major ions act as a guide in interpreting the involvement of various processes which might cause deviation in ion concentrations away from the values predicted by conservative mixing. The Δs allow hypotheses to be made about processes other than classic seawater intrusion that could account for salinization (Andersen et al., 2005). The value of Δ ion is obtained as the difference between the measured concentration in the sample analysed $[Y]_r$ and the theoretical value $[Y]_t$ deduced from ideal mixing between seawater and fresh water.

$$\Delta Y = [Y]_r - [Y]_t \text{ where} [Y]_t = [Y]_s x + [Y]_f (1-x),$$

where $[Y]_s$ is the concentration of the ion in seawater, $[Y]_f$ is the concentration of the ion in freshwater and x is the percentage of seawater calculated based on the chloride ion.

Plots of the concentrations of all the major ions in water samples were drawn. From these, the relationship between the groundwater samples, seawater (Mediterranean Sea) and fresh water end-members was analysed. The saturation indices (SI) of halite, gypsum, calcite and dolomite were also calculated using PHREEQC software (Parkhurst and Appelo, 1999). This geochemical code was also used to calculate the chemical composition of samples from the composition of the modified seawater (evaporated).

Results

Groundwater level, electrical conductivity and temperature

Under a natural regime, the groundwater level in the piezometers and multi-piezometers was close to 0.5 m asl, with no significant variation over the period of study. However, when the pumps supplying the desalination works were operating, there was an immediate response (Fig. 3). In the case of the monitoring points with their slotted length in the upper two layers of the aquifer (MP-1-1, MP-1-2, MP-2-1, MP-2-2), the piezometric head dropped between 0.5 and 1 m, with the biggest drops recorded closest to the abstraction wells. The behaviour of the piezometers slotted over their entire length (P-1 and P-2) was similar. Meanwhile, in the multipiezometers slotted through the deepest layer of the aquifer, the fall in piezometric head was up to

https://doi.org/10.1016/j.yqres.2014.04.012 Published online by Cambridge University Press

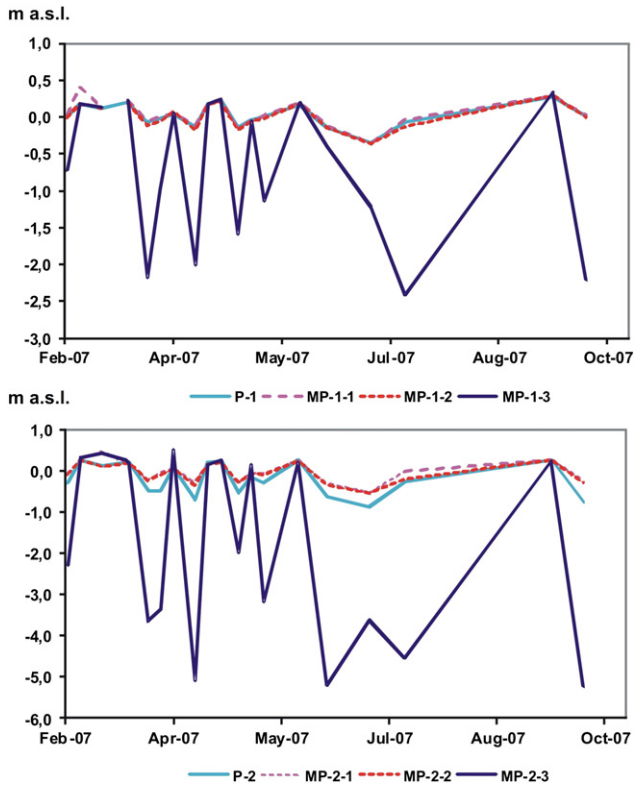

Figure 3. Evolution of groundwater level over time, as a result of pumping to supply to the desalination plant.

3 m in MP-1-3 and up to 6 m in MP-2-3 (Fig. 3). The marked variations in the extent of the fall in water table are attributed to the fact that the pumping takes water only from the lower aquifer level. This phenomenon also proves the multilayer character of this aquifer. In addition, the heterogeneity of the lithological column related to layering of materials with a very different granulometry and hydraulic behaviour contributes to the variation of water head measured in the piezometers at different depths. Layers of silts confine the aquifer affecting the groundwater level position.

Vertical electrical conductivity and temperature data, recorded from the different monitoring points before the desalination plant was operational, were used to construct a three-dimensional block of the study area (Fig. 4). Fresh water is clearly recognized in the top 20 m of the aquifer, with a net interface at 25—30 m depth, below which lies the salt water. At about 75 m depth, there is a lens of water that is more saline than seawater, which can also be distinguished in the temperature logs.

Figure 5 shows how electrical conductivity varied over the study period in the lower, saline layer of the aquifer, sometimes exceeds the conductivity measured in seawater (50—55 mS/cm). The commissioning of the desalination plant, which has been running intermittently during the study period (October 2006 to May 2008), has had its own effect on the salinity of the groundwater: during pumping, there is a clear drop in level in all the piezometers, with a partial recovery that begins when pumping ceases. The recovery is not complete and this leads, over time, to a gradual drop in the salinity. For example, conductivity at 60 m depth in piezometer P-1 went from 58 mS/cm at the beginning of the study period, to 53 mS/cm at the end. Water temperature followed the same patterns, varying between 21.5°C and 23.7°C.

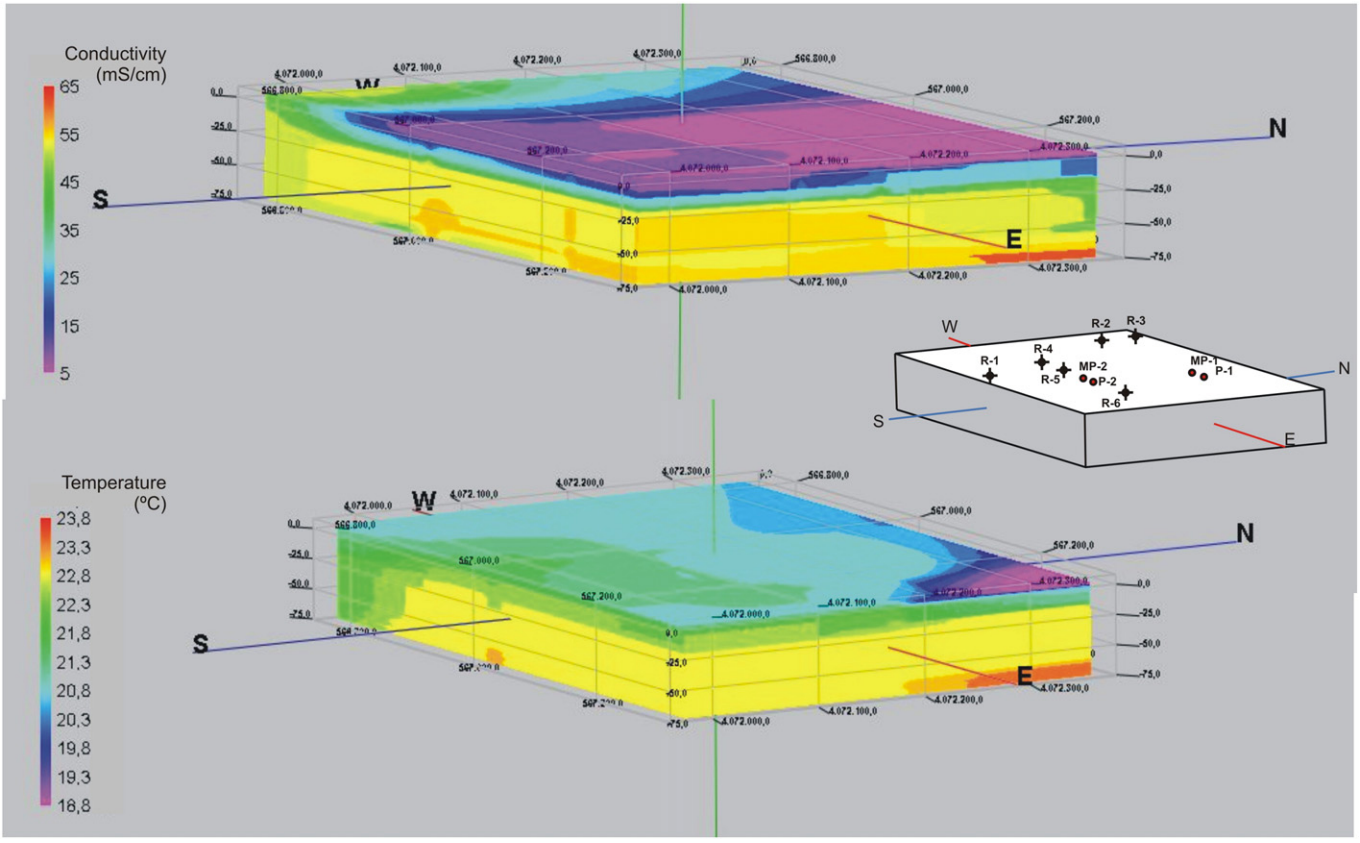

Figure 4. 3D distribution of electrical conductivity and temperature in groundwater. Location of monitoring points has been included.

https://doi.org/10.1016/j.yqres.2014.04.012 Published online by Cambridge University Press

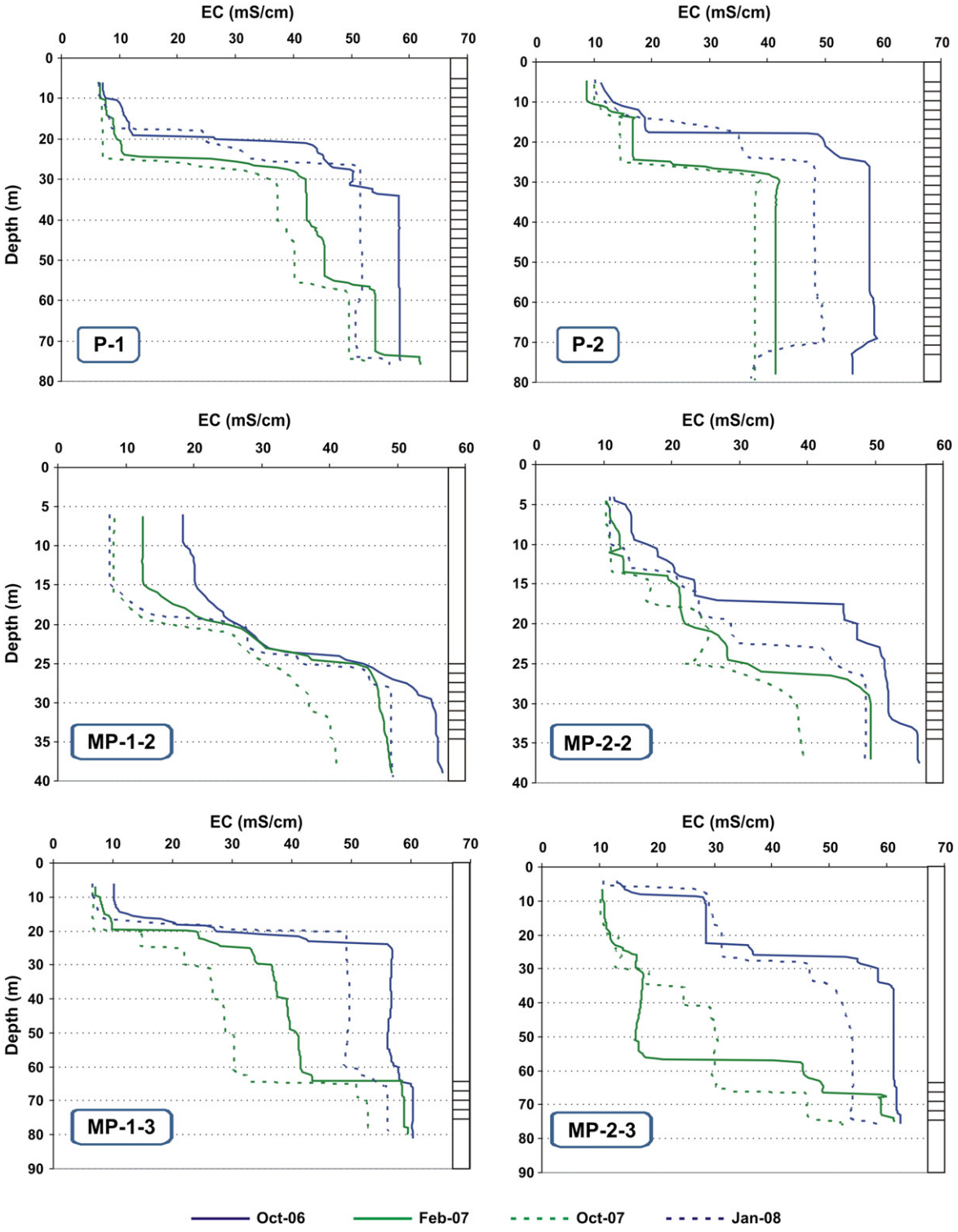

Figure 5. EC logs for piezometers in the study area (blue colour: no pumping; green colour: pumping). The screened area of the piezometers is shown.

Hydrochemistry

The physico-chemical parameters measured are presented in Table 1. Groundwater in this coastal plain is sodium-chloride type, with high salinity content. Application of cluster analysis, a multivariate technique, identified the presence of two groups of water (G1 and G2; Fig. 6). G1 comprises the samples taken in the top 30 m of the aquifer. Samples in group G2 came from below this depth. Only sample P-2(73) fell into G1, with characteristics intermediate between the two groups. Cluster analysis of the data also revealed two main groups, linked to the composition of major ions. The first cluster is linked to the ions Cl, Na, K, Mg, SO_4 and Br, whilst the second includes Ca, Sr and B (Fig. 6). The Li ion lies away from the two clusters, whilst temperature, bicarbonate and pH seem to have little bearing on the sample clusters.

Because Cl^- is considered the most conservative ion in groundwater, its concentration is plotted against the concentration of the other ions in

https://doi.org/10.1016/j.yqres.2014.04.012 Published online by Cambridge University Press

Table 1
Results of the chemical analysis of water samples. EC: electrical conductivity; SW: seawater; FW: freshwater. Location of sampling points in Figure 1.

Samples		EC	Depth	T	pH	HCO_3	Ca	Mg	Na	K	Cl	SO_4	Li	B	Sr	Br
	Code	mS/cm	m	°C		mmol/L										
P-1	P-1(8)	7.5	8	21.1	7.43	1.25	4.50	7.76	56.63	0.91	66.03	10.69	0.09	0.22	0.05	0.10
	P-1(19)	26.0	19	21.9	7.30	1.20	8.10	24.82	225.90	3.95	297.63	22.00	0.11	0.35	0.09	0.41
	P-1(32)	58.3	32	22.4	7.17	0.95	14.74	57.60	550.80	8.86	607.32	37.50	0.12	0.47	0.12	0.95
	P-1(69)	57.1	69	22.7	7.22	1.00	15.83	62.22	603.65	9.78	612.85	36.81	0.14	0.54	0.14	1.03
P-2	P-2(12)	15.2	12	22.8	7.34	1.20	6.57	15.78	122.44	2.16	146.90	14.56	0.11	0.30	0.09	0.24
	P-2(23)	40.1	23	22.9	7.22	1.30	10.63	42.11	385.75	6.57	398.28	28.00	0.09	0.39	0.11	0.68
	P-2(58)	53.7	58	23.1	7.22	0.90	13.55	56.56	545.12	9.06	595.21	38.19	0.10	0.49	0.14	0.96
	P-2(73)	43.3	73	23.5	7.41	1.00	10.47	43.77	402.73	6.72	426.28	29.97	0.09	0.40	0.10	0.70
MP-1	MP-1(8)	8.3	8	21.4	7.32	1.20	5.19	9.41	66.18	1.14	77.18	11.91	0.10	0.25	0.07	0.12
	MP-1(32)	56.9	32	21.9	7.20	0.90	15.94	60.13	570.10	9.21	595.32	35.78	0.14	0.54	0.15	1.03
	MP-1(68)	62.7	68	22.8	7.27	0.80	18.80	71.12	651.47	10.75	667.75	39.88	0.15	0.63	0.20	1.19
MP-2	MP-2(8)	12.7	8	21.6	7.51	1.20	6.32	12.32	101.04	1.73	120.79	13.47	0.10	0.27	0.08	0.17
	MP-2(30)	55.4	30	22.6	7.45	0.85	13.04	61.86	569.95	10.08	612.79	38.59	0.06	0.40	0.11	1.03
	MP-2(66)	61.9	66	21.9	7.26	0.80	17.23	66.39	644.89	11.00	636.99	37.19	0.14	0.64	0.18	1.15
SW		55.0	–	15.3	8.32	0.58	11.70	64.37	590.62	10.56	600.23	35.69	0.03	0.42	0.10	1.03
FW		3.2	–	–	7.23	4.30	2.05	3.33	19.48	0.21	24.93	1.21	0.06	0.03	0.03	0.04

the groundwater samples, and compared with seawater (Figs. 7 and 8). The first set of linked variables (Na, Mg, K, SO_4) has a linear relationship with Cl for both groups, G1 and G2 (Fig. 7). The ions that best fit the line of theoretical mixing between fresh water and seawater are Na, K and Mg. In the case of Na, all groundwater samples fell slightly below the line of theoretical fresh water–seawater mixing, clearly indicating a deficit of sodium relative to chloride. The depletion of sodium is believed to be the result of cation exchange that tends to occur in coastal aquifers when seawater intrudes a previously fresh-water aquifer (Chen and Jiao, 2007). In fact, this deficit of sodium relative to chloride compared to the theoretical mix has been used as an indicator of seawater intrusion by many researchers (Zilberbrand et al., 2001; Petalas and Lambrakis, 2006). Something similar occurs with Mg and K, though in this case, there is a gradual deviation away from the line of theoretical mixing as the samples become more saline. The SO_4 ion shows the most deviation from the theoretical straight-line relationship: samples at the fresh-water end of the scale lie away from the line of theoretical mixing, approaching it as the proportion of seawater increases. The samples that lie away from the mixing line were taken in the upper part of the aquifer and are being affected by anthropogenic pollution from the intense agricultural activity in the area.

The second cluster of ions (Ca, Sr and B) shows a very different situation to the one above (Fig. 8). In this case, the differences between samples belonging to G1 and G2 are very evident. Neither of the two clusters is closely correlated with Cl, and the relationship with Cl is particularly poor for the G2 samples. Despite the fact that this set of ions encompasses both major (Ca) and minor ions (Sr and B), the Cl concentration follows an almost identical pattern, which indicates that all of these ions are being affected by the same process. Samples belonging to G1 show a pattern of enrichment that fit a logarithmic curve of Cl concentration better than a linear one. This might indicate that the closer the sample is to seawater concentration, the less the rate of enrichment in the ion. The poor correlation with Cl of samples in group G2 indicates enrichment, and nearly all the samples have ion concentrations exceeding that of seawater. The calcium present in the G2 samples is 1.5 times that in seawater. The degree of enrichment is even greater for Sr — nearly twice that of seawater. Boron also shows a marked enrichment, with the exception of one sample (which is slightly impoverished in B).

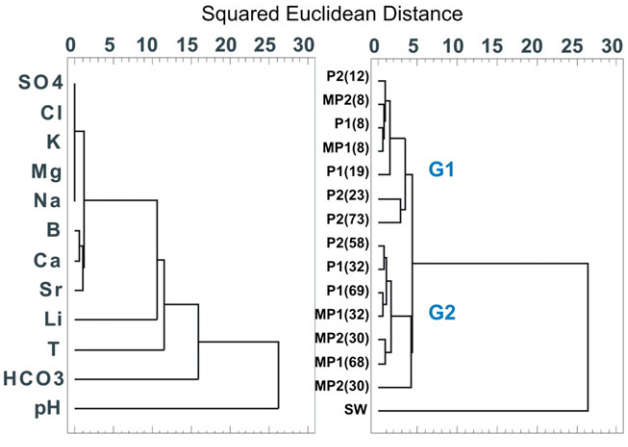

Figure 6. Cluster diagrams of variables and observations based on squared Euclidean distance (numbers in brackets are depths of groundwater samples).

In the case of comparing Li (separated from the other ions in the cluster analysis; Fig. 6) to Cl, there are certain similarities to the Ca–Sr–B cluster of ions described above. The sample groups G1 and G2 are also easily distinguished. Samples belonging to G1 show concentrations of 0.6—0.8 mg/L, with the highest Li concentrations being recorded in the samples of intermediate salinity. The Li–Cl correlation is nil or poor in the case of the G2 samples. Both the G1 and G2 samples are clearly enriched in Li compared to seawater, between 3 and 5 times, respectively. These high Li concentrations suggest an origin that is not seawater. One sample has characteristics very much like seawater and this sample was taken at a depth of 30 m in the MP-2 cluster.

Calculation of percentage SW–FW mixing rate

The percentage of seawater (SW) was determined on the basis of Cl concentration, a conservative ion in the mixing process between fresh water (FW) and seawater (Table 2). In the G1 samples, the percentage of seawater oscillated between 7 and 70%. In general, the higher proportions correspond to samples taken at greater depth. On the other hand, water samples in group G2 are calculated to contain between 99 and 116% of seawater. This suggests that the majority of this water have higher Cl concentrations than seawater. One explication of the high concentration is that these waters have been subject to evaporation.

Since the ^{18}O isotope is also conservative, it was also used for calculating the proportion of seawater in the samples (Stuyfzand and Stuurman, 2006). Our results indicate that the percentage of seawater is between 16 and 61% in samples belonging to G1, similar proportions to those calculated from the chloride ion. Nevertheless, the results for G2 samples are very different, with values clearly lower, close to 65%, with the exception of sample MP-2(30) which indicates 91% seawater (Table 2).

This difference in the chloride and ^{18}O indicates that the initial chemical composition has been modified. If this modification process

https://doi.org/10.1016/j.yqres.2014.04.012 Published online by Cambridge University Press

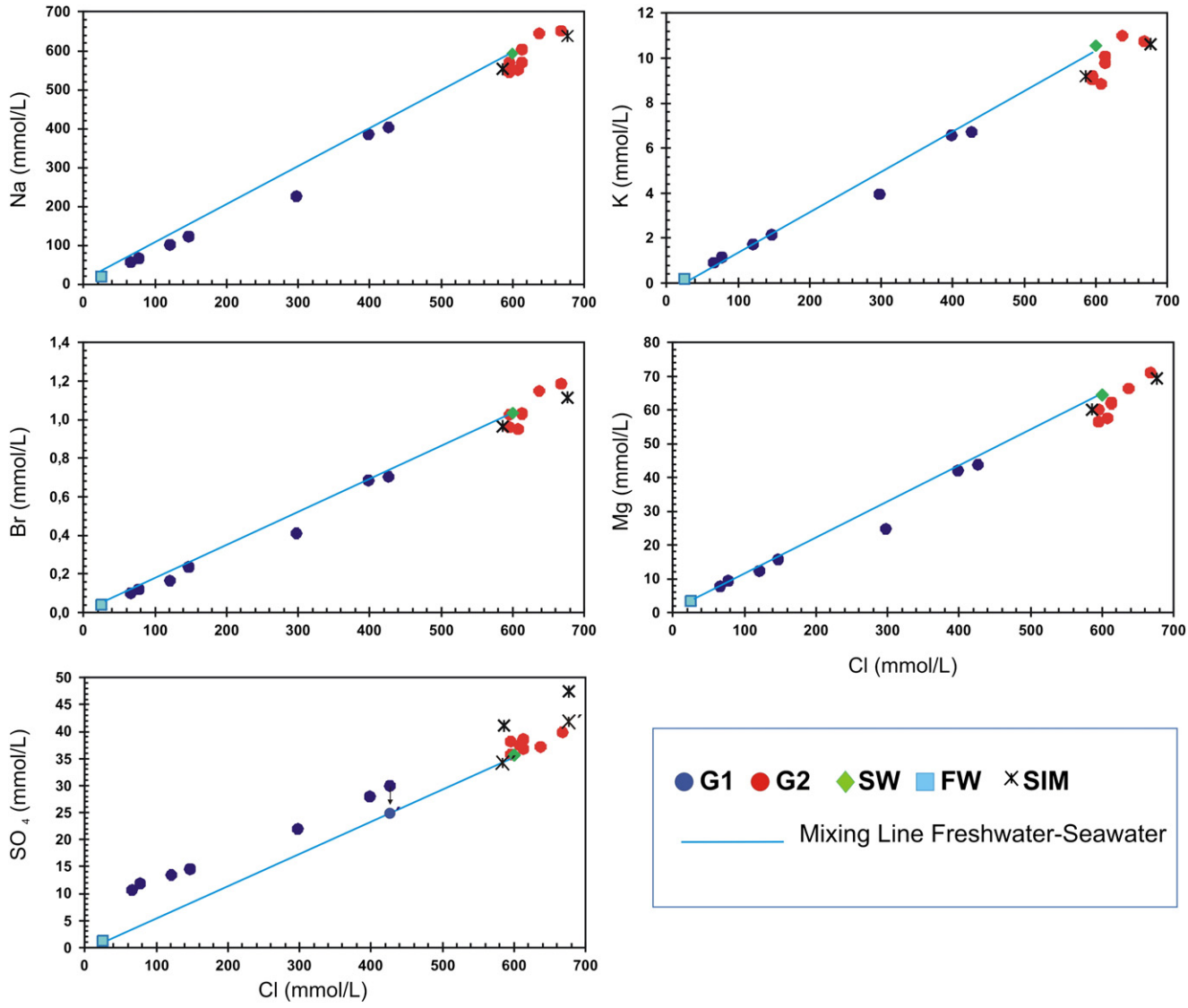

Figure 7. Hydrochemical relationships between selected ions of groundwater samples (G1, G2) and seawater composition (SW). Mixing line between seawater (SW) and fresh water (FW) is plotted for reference. Cross symbol (SIM) represents the results obtained from hydrogeochemical simulations (see Section Hydrogeochemical modelling).

were evaporation, the ion concentrations in the samples would have been more affected than their isotope composition.

The deuterium and ^{18}O isotopic data of the investigated waters are reported in Table 2. The delta values with respect to VSMOW range from −7.3 to +1.1‰ for $\delta^{18}O$ and from −51.9 to +11.2‰ for $\delta^{2}H$. The relationship between deuterium and ^{18}O provides a clear picture of the linear mixing between the two poles of fresh groundwater at one end and seawater at the other (Gat and Gonfiantini, 1981; Payne, 1983; Gonfiantini and Araguas, 1988; Ho et al., 1992; Zakhem and Hafez, 2007). The isotope composition of the samples in given in Figure 9A, which shows a gap between the samples in G2 and the Global Meteoric Water Line (GMWL) or Western Mediterranean Meteoric Water Line (MMWL). There is an increasing trend in both $\delta^{18}O$ and $\delta^{2}H$ in the groundwater samples, corresponding to the increasing salinity from fresh water to brine. This reflects the influence of evaporation as a major process increasing salinity. Most samples from the group, G1, lie on the meteoric water line, though two samples are grouped with the G2 samples. It is possible that these two, in common with all the samples in G2, have been subject to evaporation. It is easy to see that one of the samples has a composition similar to seawater.

Based on the chloride–^{18}O relationship (Fig. 9B), we can see how the less saline samples respond to mixing with present-day seawater, whilst evaporation (leading to a loss of water far in excess of that supplied from precipitation) may explain the high Cl content and the anomalous $\delta^{18}O$ of these samples. If the samples in the G1 group with Cl concentrations above 400 mmol/L were evaporated by 25−35%, they would be incorporated in the G2 group, as we will demonstrate below.

Hydrogeochemical modelling

Samples in group G2 have a chemical composition in which the majority of ions are present in concentrations higher than that of seawater. To check if the changes in chemistry are due to a process of evaporation, hydrogeochemical modelling was undertaken. We began by considering a sample of type G1, which, according to the ^{18}O analysis, contains a similar percentage of seawater to samples of type G2. The modelling began with water similar to the concentration of sample P2(73), which shows characteristics intermediate between the two sample groups and which contains about 60% seawater, similar to the proportion found in type G2 (Table 2).

Modelling used the PHREEQC code (Parkhurst and Appelo, 1999). All sampled groundwaters had negative SIs with respect to calcite, dolomite, gypsum and halite, so they are subsaturated with respect to these minerals. Different percentages of evaporation were applied to

https://doi.org/10.1016/j.yqres.2014.04.012 Published online by Cambridge University Press

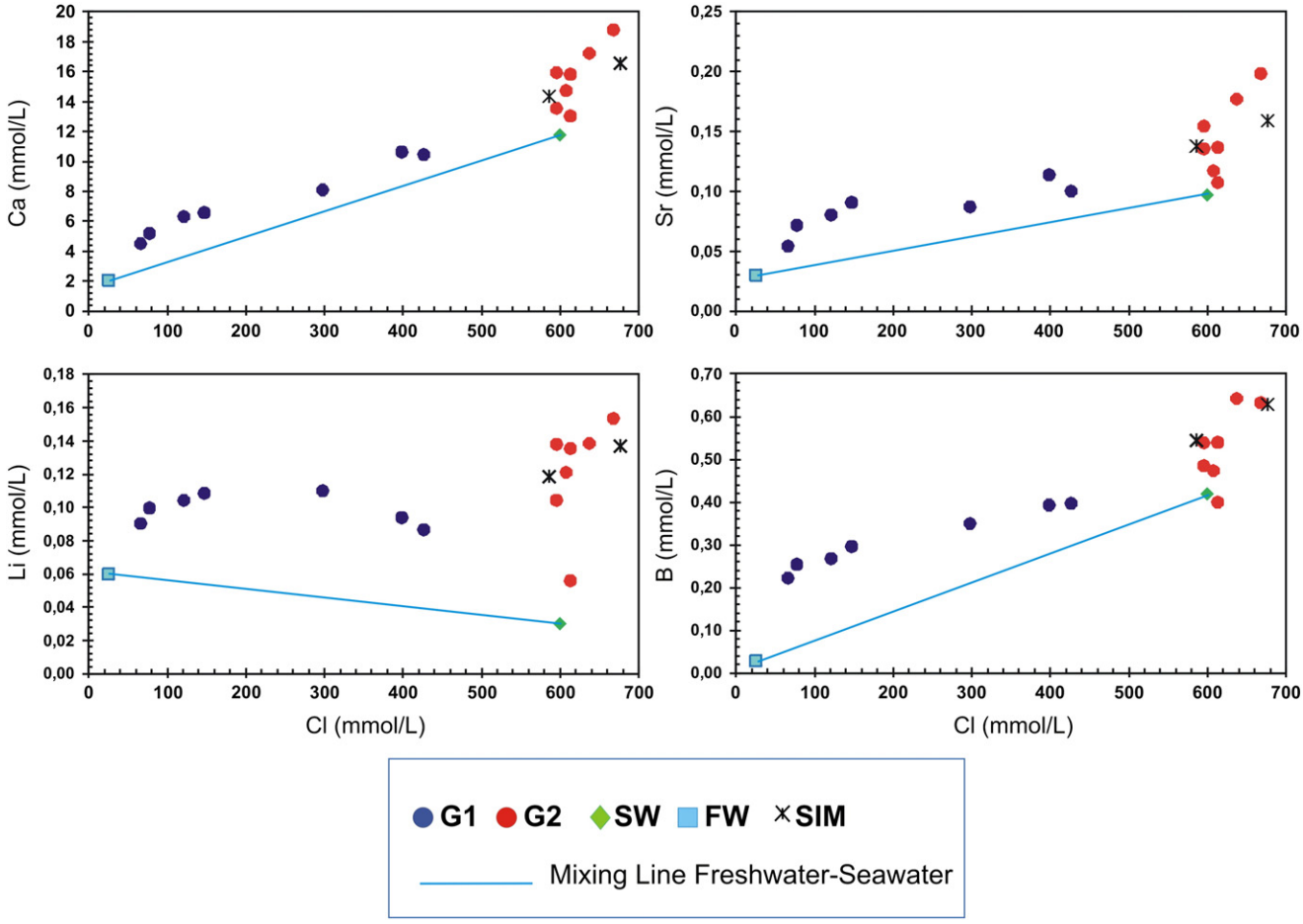

Figure 8. Hydrochemical relationships between selected ions (Ca, Sr, Li and B) and Cl, for groundwater samples (G1, G2) and seawater composition (SW). Cross symbol (SIM) represents the results from hydrogeochemistry modelling (see Section Hydrogeochemical modelling).

the original sample until the chemical concentrations similar to the G2 type were obtained (Fig. 10). The rates of evaporation that gave the best result are between 25 and 35%, which produced ion concentrations for Na, K, Mg and Br that were very similar to samples in this group (Fig. 7). For SO_4, the results of the modelling were not optimal. The aquifer has suffered anthropogenic pollution from the intense agricultural activity in the area, which contributes an additional source of SO_4. This would explain why samples taken closer to the ground surface are plotted further from the line of theoretical mixing of fresh water–seawater (Fig. 7). If the contamination effect that have occurred in the last years

Table 2
Isotopic data of samples and percentage of seawater calculated from isotopic content.

SAMPLE		Group	^{18}O	^{2}H	Seawater
	Code		‰		%
P-1	P-1(8)	G1	−6.01	−34.5	16
	P-1(19)	G1	−5.29	−32.2	24
	P-1(32)	G2	−2.18	−14.6	61
	P-1(69)	G2	−1.88	−11.5	65
P-2	P-2(12)	G1	−5.39	−31.5	23
	P-2(23)	G1	−2.57	−15.9	57
	P-2(58)	G2	−1.53	−9.3	69
	P-2(73)	G1	−2.24	−14.1	61
MP-1	MP-1(8)	G1	−5.83	−33	18
	MP-1(32)	G2	−2.31	−14.2	60
	MP-1(68)	G2	−1.94	−11.6	64
MP-2	MP-2(8)	G1	−5.4	−30.2	23
	MP-2(30)	G2	0.31	2.8	91
	MP-2(66)	G2	−1.93	−9.8	64
SW		–	1.06	11.2	–

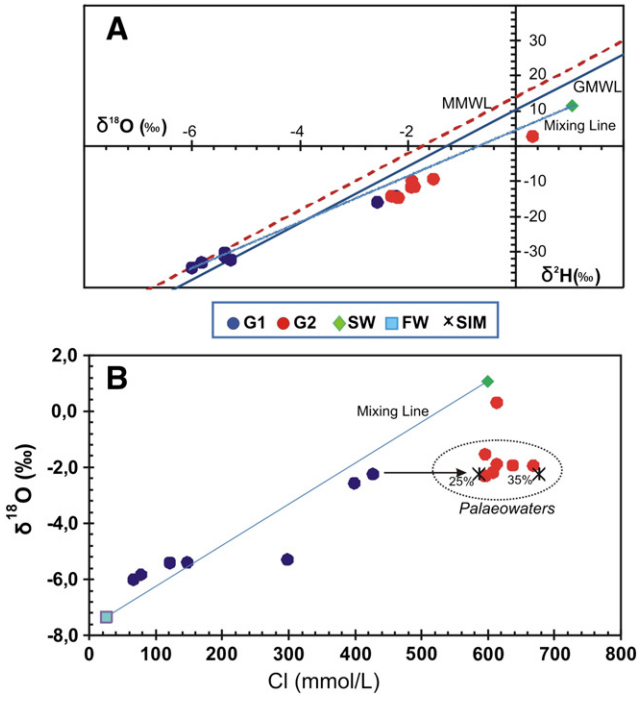

Figure 9. (A) Relationship between $\delta^{18}O$ and $\delta^{2}H$ in water samples (relative to VSMOW). The global meteoric water line (GMWL) corresponds to Craig (1961) and the Western Mediterranean meteoric water line (MMWL) to Celle-Jeanton et al. (2001). (B) Plot of $\delta^{18}O$ vs. Cl. Simulated water samples have been included in this graph (see Section Hydrogeochemical modelling).

https://doi.org/10.1016/j.yqres.2014.04.012 Published online by Cambridge University Press

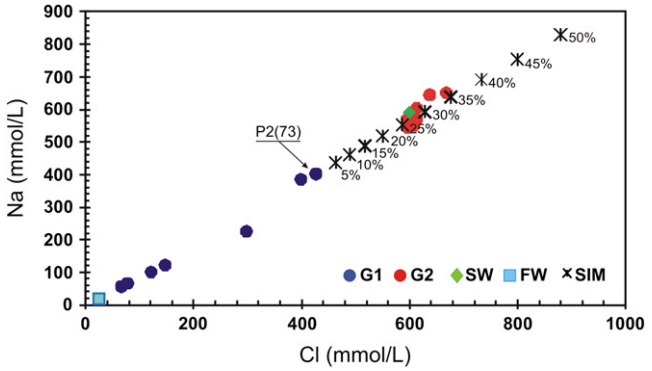

Figure 10. Relationship between Cl and Na of samples taken and simulated waters assuming different evaporation rates. The simulations were performed using PHREEQC.

is eliminated, by moving the sample towards the line of theoretical mixing and rerunning the simulation, the result is similar to that in the samples in group G2. In Figure 7, the graph corresponding to SO_4 vs Cl includes the points corresponding to the concentrations obtained from the first simulation (*) and from a second simulation in which the effect of surface pollution has been removed (*′).

For the other ions associated in the cluster analysis (Ca, Sr and B), the simulations – although not as good as before – fit reasonably well to those measured in the G2 samples (Fig. 8). The poorer fit could be due to the concurrence of other processes, such as ion exchange, which would affect the G2 samples more because of the longer water–rock contact time. Na would have been involved in the ion exchange but the high concentrations of this ion mean that the effect is not as evident. The calculated ion deltas – positive for Ca and negative for Na – corroborate this idea (Daniele et al., 2011).

The Li ion merits special mention. Its elevated concentration, in samples of both high and low salinities, is greater than in the seawater sample. This is due to the input from the volcanic outcrops (mainly andesites) in the vicinity of the study area; the possibility of a hydrothermal origin or of a link to a continental salt spring has been discounted (Price et al., 2000; Munk et al., 2011). Only sample MP-2(30) has a Li composition similar to seawater, which is explained by the fact that it is composed of 90% of seawater (according to its oxygen-18 content). Figure 9B shows the results of the modelling of the 25—35% evaporation rates in terms of the relation $\delta^{18}O$—chloride ratio; it is clear that these simulations are consistent with the results obtained based on the concentrations of other ions.

Interpretation of the paleoenvironment

There is a close link between geological evolution, water quality and what is still observable today. As a result, it is possible to reconstruct the environment that prevailed from the Holocene by interpreting hydrogeochemical information. In this study we have reconstructed palaeowaters by means of simulations based on various rates of evaporation. The rates of evaporation modelled here would imply that the water of type G2 was surface water. Based on the percentage of seawater, calculated using the concentration of ^{18}O in the samples, we can affirm that these waters possess characteristics similar to a fresh water—seawater mixing zone, containing 60—70% seawater. This water was then modified through cation exchange, becoming enriched in ions like Ca, Sr and B, with the consequent drop in Na. Weathering and leaching of minerals from the volcanic rocks in the landscape immediately around the aquifer would have markedly increased Li concentrations in the groundwater.

The next step is to postulate the kinds of paleoenvironment that combine evaporation and ionic concentration. A candidate in this case would be a coastal lagoon located just beyond the north-eastern edge of the study area (Fig. 1). Whilst the lagoon has now partially disappeared, sediment characteristic of this type of environment has been identified in this location; this lagoon would have been active between 8 and 3 ka (Goy et al., 1998). The geological evolution of this lagoon has been established by geomorphological analysis and radiometric dating conducted in the area by other authors. The lagoon is partially fed by alluvial fans from Sierra de Gata ranges. Three groups of fans occur in this area. These were dated based on their relationship with the marine terraces, by means of the stratigraphic study and Th/U dating of the coastal sediments (Hillaire-Marcel et al., 1986). The two first and main aggradational phases are coincident with glacial periods (>ca. 135 ka and ca. 85–10 ka) during which a sedimentation phase occurs. The last phase of alluvial fan development corresponds to middle-upper Holocene. Meanwhile, during interglacial periods their partial dissection occurs (Harvey et al., 1999). The littoral drift develops a coastal bar enclosing a lagoon, so that this generation of fans has no relationship to marine base levels. On the Cabo de Gata west-coast fans, base level has varied very little. The range in elevation from the surface of the lagoon during high sea levels to the flat floor of the lagoon during low sea levels was insufficient to have had any major influence on the geomorphology of the fans (Harvey, 2002). The beach and lagoon have a depositional record of about 6 ka (Goy et al., 1996; Jalut et al., 2000). Three periods in the evolution of the lagoon have been distinguished with sediment cores (Reicherter and Becker-Heidmann, 2009). The initial stage is the predominantly alluvial fan phase, which commenced during Pleistocene times (Harvey et al., 1999), followed by an intermediate beach phase from approximately 6 to 3 ka, and from then on a marsh lagoon developed. Currently part of this lagoon system remains active in its eastern part, and is located 2 km east of the study area (Fig. 1).

The water held in this lagoon would have been denser than the mixing water in the aquifer. As a result, there would have been a tendency for the denser surface water to infiltrate into the aquifer and to sink to its base, so creating the waters identified in this study as type G2 (Fig. 11). This water would have continued to interact with the aquifer matrix rock, increasing the overall cation exchange. A similar scenario to the one proposed here has been described to explain the presence of highly saline groundwater in a coastal marine environment adjacent to a coastal lagoon, which was used as a salt pan during the last century (1925–1975) (Alhama et al., 2012).

Geological evolution during the Quaternary was dominated by a continuous transgression of the sea and progressive silting up of the coastal plain. The rise in sea level over the last Flandrian Transgression would have favoured marine intrusion in many coastal aquifers (Dever et al., 2001; Stuyfzand and Stuurman, 2006; Vandenbohede and Lebbe, 2012; Giambastiani et al., 2013; Khaska et al., 2013). At the peak of the transgression, sea level on the Mediterranean coast of the southeastern Iberian Peninsula would have been up to 1 m higher than in the present-day (Goy et al., 2003) and, in our study area, the paleo-coastline would have lain almost a kilometre further inland (Goy et al., 1998). When the coastline became established in its current position, this would have flushed the upper, unconfined aquifer levels. Accordingly, the water in this part of the aquifer is between 10 and 60% seawater. The rates of evaporation calculated (25—35%) would be indicative of a wetter, more temperate climate during the middle Holocene than today. These climatic conditions have also been identified from the palynological record (Pantaleón-Cano et al., 1996; Jalut et al., 2000).

Human activity would have been the cause of the latest modification of the chemistry and hydrodynamics of the aquifer. Irrigation returns from greenhouse crops have infiltrated the aquifer leading to sulphate pollution of the waters of type G1; moreover, the abstractions to supply the desalination plant take the most saline waters from the base of the aquifer, leading to a gradual reduction in groundwater salinity. The presence of a fracture parallel to the present-day coastline could also be limiting the ingress of the saltwater wedge beneath the aquifer, so that all the water being abstracted could be fossil water, type G2,

https://doi.org/10.1016/j.yqres.2014.04.012 Published online by Cambridge University Press

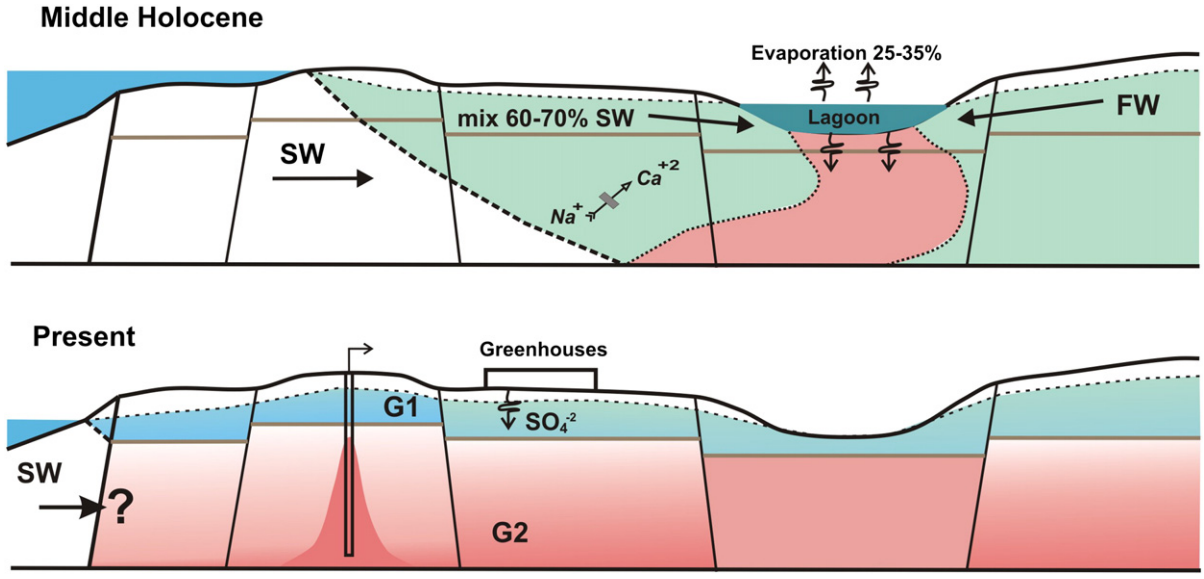

Figure 11. Scheme of evolution of the aquifer during the Middle Holocene. G1 and G2: groundwater types, FW: fresh water, SW: seawater.

hence its higher salt concentration than in present-day seawater (Fig. 11).

Conclusions

Two clearly differentiated water types occur in the Cabo de Gata aquifer. The first (G1) contains between 10 and 60% seawater and characterises the upper, unconfined aquifer. The G1 waters have undergone slight modification, mainly as a result of ion exchange, namely adsorption of Na and liberation of Ca. In some mineral structures, ions like Sr and B take the same position as Ca, and so are involved in the ion exchange process. The elevated concentration of Li is attributed to inflows of continental water rich in this element, which comes from weathering of the predominantly volcanic reliefs in this area. The second group (G2) contains a higher percentage of seawater (60−70%), though the overall salinity is greater than that of seawater, due to evaporation. This evaporation must have occurred in a coastal lagoon environment during the middle Holocene, identified by Goy et al. (1998) from sediments preserved to the northeast of the study area. Later, the greater density of the water meant that it infiltrated to the lower part of the aquifer. Hydrogeochemical modelling to simulate the generation of G2 type waters assuming evaporation of G1 water fitted quite well with values measured in the field. The ions showing the poorest fit correspond to ions that have been enriched due to interaction between the groundwater and the host rock. Abstraction of water from the aquifer is causing a generalized drop in salinity, indicating that there is little hydraulic connection to the sea. Thus, it is clear that these abstractions are of paleowaters, whose characteristics were developed in a coastal lagoon context during the Holocene as a consequence of the Flandrian Transgression. The rate of evaporation calculated based on the hydrogeochemical modelling allows the climatic conditions that prevailed during the Flandrian Transgression to be identified.

References

Akouvi, A., Dra, M., Violette, S., de Marsily, G., Zuppi, G.M., 2008. The sedimentary coastal basin of Togo: example of a multilayered aquifer still influenced by a palaeo-seawater intrusion. Hydrogeology Journal 16, 419–436.

Alhama, I., Rodríguez-Estrella, T., Alhama, F., 2012. Hydric restoration of the Agua Amarga saltmarsh (SE Spain) affected by abstraction from the underlying coastal aquifer. Water Resources Management 26, 1763–1777.

Andersen, M., Jacobsen, V., Postma, D., 2005. Geochemical processes and solute transport at the seawater/freshwater interface of a sandy aquifer. Geochimica et Cosmochimica Acta 69, 3979–3994.

Appelo, C.A.J., Postma, D., 2005. Geochemistry, Groundwater and Pollution, 2nd edn. AA Balkema, Rotterdam (649 pp.).

Avrahamov, N., Sivan, O., Yechieli, Y., Lazar, B., Levenberg, O., 2010. Characterization and dating of saline groundwater in the Dead Sea area. Radiocarbon 52 (3), 1123–1140.

Carreira, P.M., Marques, J.M., Nunes, D., 2014. Source of groundwater salinity in coastline aquifers based on environmental isotopes (Portugal): natural vs. human interference. A review and reinterpretation. Applied Geochemistry 41, 163–175.

Celle-Jeanton, H., Travi, Y., Blavoux, B., 2001. Isotopic typology of the precipitation in the Western Mediterranean region at three different time scales. Geophysical Research Letters 28, 1215–1218.

Cheikh, N.B., Zouari, K., Abidi, B., 2012. Geochemical and isotopic study of paleogroundwater salinization in southeastern Tunisia (Sfax basin). Quaternary International 257, 34–42.

Chen, K.P., Jiao, J.J., 2007. Seawater intrusion and aquifer freshening near reclaimed coastal area of Shenzhen. Water Science & Technology: Water Supply 7 (2), 137–145.

Craig, H., 1961. Isotopic variations in meteoric waters. Science 133, 1702–1703.

Custodio, E., 1997. Studying, monitoring and controlling seawater intrusion in coastal aquifers. Guidelines for Study, Monitoring and Control, FAO Water Reports No. 11, pp. 7–23.

Custodio, E., 2010. Coastal aquifers of Europe: an overview. Hydrogeology Journal 18, 269–280.

Daniele, L., Vallejos, A., Sola, F., Corbella, M., Pulido-Bosch, A., 2011. Hydrogeochemical processes in the vicinity of a desalination plant (Cabo de Gata, SE Spain). Desalination 277, 338–347.

Darling, W.G., Edmunds, W.M., Smedley, P.L., 1997. Isotopic evidence for palaeowaters in the British Isles. Applied Geochemistry 12, 813–829.

Dever, L., Travi, Y., Barbecot, F., Marlin, C., Gibert, E., 2001. Evidence for palaeowaters in the coastal aquifers of France. Geological Society of London, Special Publication 189, 93–106.

Edmunds, W., Milne, C.J., 2001. Palaeowaters in coastal Europe: evolution of groundwater since late Pleistocene. Geological Society of London, Special Publication 189.

Fass, T., Cook, P., Stieglitz, T., Herczeg, A., 2007. Development of saline ground water through transpiration of sea water. Ground Water 45 (6), 703–710.

Faye, S., Maloszewski, P., Stichler, W., Trimborn, P.S.C., Gaye, C.B., 2005. Groundwater salinization in the Saloum (Senegal) delta aquifer: minor elements and isotopic indicators. The Science of the Total Environment 343, 243–259.

Frank, T.D., Gui, Z., Science Team, A.N.D.R.I.L.L.S.M.S., 2010. Cryogenic origin for brine in the subsurface of southern McMurdo Sound, Antarctica. Geology 38 (7), 587–590.

Gat, J.R., Gonfiantini, R., 1981. Stable isotope hydrology: deuterium and oxygen-18 in the water cycle. Technical Report Series No. 210. IAEA, Vienna.

Gattacceca, J.C., Vallet-Coulomb, C., Mayer, A., Claude, C., Radakovitch, O., Conchetto, E., Hamelin, B., 2009. Isotopic and geochemical characterization of salinization in the shallow aquifers of a reclaimed subsiding zone: the southern Venice Lagoon coastland. Journal of Hydrology 378, 46–61.

Giambastiani, B.M., Colombani, N., Mastrocicco, M., Fidelibus, M.D., 2013. Characterization of the lowland coastal aquifer of Comacchio (Ferrara, Italy): hydrology, hydrochemistry and evolution of the system. Journal of Hydrology 501, 35–44.

Gonfiantini, R., Araguas, L., 1988. Los isótopos ambientales en el estudio de la intrusión marina. Tecnología de la intrusión en acuíferos. IGME, Madrid, pp. 135–190.

Goy, J.L., Zazo, C., Dabrio, C.J., Lario, J., Borja, F., Sierro, F.J., Flores, J.A., 1996. Global and regional factors controlling changes of coastlines in Southern Iberia (Spain) during the Holocene. Quaternary Science Reviews 15, 773–780.

Goy, J.L., Zazo, C., Dabrio, J.C., Baena, J., Harvey, A.M., Silva, P.G., González, F., Lario, J., 1998. Sea level and climate change in the Cabo de Gata lagoon (Almeria) during the last 6500 yr BP. INQUA. MBSS. Newsletter 20, 11–18.

https://doi.org/10.1016/j.yqres.2014.04.012 Published online by Cambridge University Press

Goy, J.L., Zazo, C., Dabrio, J.C., 2003. A beach-ridge progradation complex reflecting periodical sea-level and climate variability during the Holocene (Gulf of Almería, Western Mediterranean). Geomorphology 50, 251–268.
Han, D., Kohfahl, C., Song, X., Xiao, G., Yang, J., 2011. Geochemical and isotopic evidence for palaeo-seawater intrusion into the south coast aquifer of Laizhou Bay, China. Applied Geochemistry 26, 863–883.
Harvey, A.M., 2002. The role of base-level changes in the dissection of alluvial fans: case studies from southeast Spain and Nevada. Geomorphology 45, 67–87.
Harvey, A.M., Silva, P.G., Mather, A.E., Goy, J.L., Stokes, M., Zazo, C., 1999. The impact of Quaternary sea-level and climatic change on coastal alluvial fans in the Cabo de Gata ranges, southeast Spain. Geomorphology 28, 1–22.
Hillaire-Marcel, C., Carro, O., Causse, C., Goy, J.L., Zazo, C., 1986. Th/U dating of *Strombus bubonius*-bearing marine terraces in southest Spain. Geology 14, 613–616.
Ho, H.D., Aranyossy, J.F., Louvat, D., Hua, M.Q., Nguyen, T.V., 1992. Environmental isotope study related to the origin, salinization and movement of groundwater in the Mekong Delta (Viet Nam). IAEA-SM-319/38. IAEA, Vienna.
Hodgkinson, J., Cox, M.E., McLoughlin, S., 2007. Groundwater mixing in a sand–island freshwater lens: density-dependent flow and stratigraphic controls. Australian Journal of Earth Sciences 54 (7), 927–946.
Jalut, G., Amat, A.E., Bonnet, L., Gauguelin, Th., Fontugne, M., 2000. Holocene climatic changes in the western Mediterranean, from south-east France to south-east Spain. Palaeogeography, Palaeoclimatology, Palaeoecology 160, 255–290.
Kafri, U., Yechieli, Y., 2012. The relationship between current and paleo groundwater base-levels. Quaternary International 257, 83–96.
Kharroubi, A., Gzam, M., Jedoui, Y., 2012. Anthropogenic and natural effects on the water and sediments qualities of costal lagoons: case of the Boughrara Lagoon (Southeast Tunisia). Environmental Earth Sciences 67, 1061–1067.
Khaska, M., La Salle, C., Lancelot, J., ASTER team, Mohamad, A., Verdoux, P., Noret, A., Simler, R., 2013. Origin of groundwater salinity (current seawater vs. saline deep water) in a coastal karst aquifer based on Sr and Cl isotopes. Case study of the La Clape massif (southern France). Applied Geochemistry 37, 212–227.
Kooi, H., Groen, J., Leijnse, A., 2000. Modes of seawater intrusion during transgression. Water Resources Research 36 (12), 3581–3590.
Levanon, E., Yechieli, Y., Shalev, E., Friedman, V., Gvirtzman, H., 2013. Reliable monitoring of the transition zone between fresh and saline waters in coastal aquifers. Groundwater Monitoring & Remediation 33, 101–110.
Lu, C., Chen, Y., Zhang, C., Luo, J., 2013. Steady-state freshwater–seawater mixing zone in stratified coastal aquifers. Journal of Hydrology 505, 24–34.
Manzano, M., Custodio, E., Loosli, H., Cabrera, M.C., Riera, X., Custodio, J., 2001. Palaeowater in coastal aquifer of Spain. Geological Society, Special Publication 189, 107–138.
Munk, L.A., Bradley, D.C., Hynek, S.A., Chamberlain, C.P., 2011. Origin and evolution of Li-rich Brines at Clayton Valley, Nevada, USA. American Geophysical Union, Fall Meeting 2011.
Pantaleón-Cano, J., Yll, E.I., Pérez-Obiol, R., Roure, J.M., 1996. Las concentraciones polínicas en medios semiáridos. Su importancia en la interpretación de la evolución del paisaje. In: Ramil-Rego, P., Fernández Rodríguez, C., Rodríguez Guitian, M. (Eds.), Biogeografía Pleistocena-Holocena de la Península Ibérica. Xunta de Galicia, Santiago de Compostela, pp. 215–226.
Parkhurst, D.L., Appelo, C.A.J., 1999. User's guide to PHREEQC (version 2) — a computer program for speciation, batch-reaction, one-dimensional transport, and inverse geochemical calculations. U.S. Geological Survey Water-Resources Investigations Report 99–4259 (312 pp.).
Payne, B.R., 1983. Groundwater salinization: guidebook on nuclear techniques in hydrology. Technical Report Series No. 91. IAEA, Vienna.
Petalas, C.P., Diamantis, I.B., 1999. Origin and distribution of saline groundwaters in the upper Miocene aquifer system, coastal Rhodope area, northeastern Greece. Hydrogeology Journal 7, 305–316.
Petalas, C., Lambrakis, N., 2006. Simulation of intense salinization phenomena in coastal aquifers — the case of the coastal aquifers of Thrace. Journal of Hydrology 324, 51–64.
Post, V., 2003. Groundwater Salinization Processes in the Coastal Area of the Netherlands Due to Transgressions During the Holocene. (Ph.D. Thesis) Free University, The Netherlands.
Price, J.G., Lechler, P.J., Lear, M.B., Giles, T.F., 2000. Possible volcanic source of lithium in brines in Clayton Valley, Nevada. In: Cluer, J.K., Price, J.G., Struhsacker, E.M., Hardyman, R.F., Morris, C.L. (Eds.), Geology and ore deposits 2000: the Great Basin and beyond: Geological Society of Nevada Symposium Proceedings, May 15–18, 2000, Reno, pp. 241–248.
Re, V., Sacchi, E., Martin-Bordes, J.L., Aureli, A., El Hamouti, N., Bouchnan, R., Zuppi, G.M., 2013. Processes affecting groundwater quality in arid zones: the case of the Bou-Areg coastal aquifer (North Morocco). Applied Geochemistry 34, 181–198.
Reicherter, K., Becker-Heidmann, P., 2009. Tsunami deposits in the western Mediterranean: remains of the 1522 Almeria earthquake? Geological Society, London, Special Publications 316 (1), 217–235.
Sánchez-Martos, F., Molina-Sánchez, L., Gisbert-Gallego, J., 2014. Groundwater–wetlands interaction in coastal lagoon of Almería (SE Spain). Environmental Earth Sciences 71, 67–76.
Sola, F., Vallejos, A., Moreno, L., López Geta, J.A., Pulido Bosch, A., 2013. Identification of hydrogeochemical process linked to marine intrusion induced by pumping of a semiconfined mediterranean coastal aquifer. International Journal of Environmental Science and Technology 10, 63–76.
Stuyfzand, P.J., Stuurman, R.J., 1994. Recognition and genesis of various brackish to hypersaline groundwaters in The Netherlands. Proc. 13th Salt Water Intrusion Meeting, June 1994, Cagliari Italy. Univ. Cagliari, Fac. Engineering, pp. 125–136.
Stuyfzand, P.J., Stuurman, R.J., 2006. Origin, distribution and chemical mass balances of non-anthropogenic, brackish and (hyper)saline groundwaters in the Netherlands. Proc. 1st SWIM-SWICA Joint Saltwater Intrusion Conference, Cagliari, Italy, pp. 151–164.
Sukhija, B.S., Varma, V.N., Nagabhushanam, P., Reddy, D.V., 1996. Differentiation of palaeomarine and modern seawater intruded salinities in coastal groundwaters (of Karaikal and Tanjavur, India) based on inorganic chemistry, organic biomarker fingerprints and radiocarbon dating. Journal of Hydrology 174, 173–201.
Været, L., Leijnse, A., Cuamba, F., Haldorsen, S., 2012. Holocene dynamics of the salt–fresh groundwater interface under a sand island, Inhaca, Mozambique. Quaternary International 257, 74–82.
Vandenbohede, A., Lebbe, L., 2012. Groundwater chemistry patterns in the phreatic aquifer of the central Belgian coastal plain. Applied Geochemistry 27, 22–36.
Wang, Y., Jiao, J.J., 2012. Origin of groundwater salinity and hydrogeochemical processes in the confined Quaternary aquifer of the Pearl River Delta, China. Journal of Hydrology 438–439, 112–124.
Werner, A.D., Bakker, M., Post, V., Vandenbohede, A., Lu, C., Ataie-Ashtiani, B., Simmons, C. T., Barry, D.A., 2013. Seawater intrusion processes, investigation and management: recent advances and future challenges. Advances in Water Resources 51, 3–26.
Yechieli, Y., Shalev, E., Wollman, S., Kiro, Y., Kafri, U., 2010. Response of the Mediterranean and Dead Sea coastal aquifers to sea level variations. Water Resources Research 46, W12550.
Zakhem, B.A., Hafez, R., 2007. Environmental isotope study of seawater intrusion in the coastal aquifer (Syria). Environmental Geology 51, 1329–1339.
Zilberbrand, M., Rosenthal, E., Shachnai, E., 2001. Impact of urbanization on hydrochemical evolution of groundwater and on unsaturated-zone gas composition in the coastal city of Tel Aviv, Israel. Journal of Contaminant Hydrology 50 (3–4), 175–208.

https://doi.org/10.1016/j.yqres.2014.04.012 Published online by Cambridge University Press